Analytical Methods

Accepted Manuscript

This article can be cited before page numbers have been issued, to do this please use: E. D. Donarski, D. R. Luedeka and B. J. Venton, *Anal. Methods*, 2026, DOI: 10.1039/D6AY00403B.

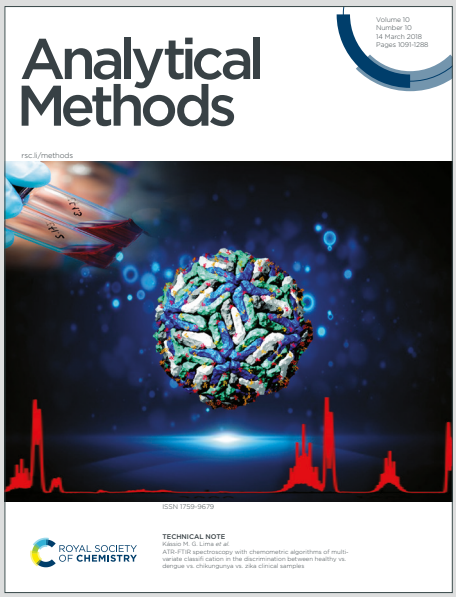

ROYAL SOCIETY OF CHEMISTRY

rsc.li/methods

View Article Online
DOI: 10.1039/D6AY00403B

Blue Light Enhances Background Current and Dopamine Sensitivity of Carbon-Fiber Microelectrodes During Fast-Scan Cyclic Voltammetry

Eric D. Donarski[1], David R. Luedeka[1], and B. Jill Venton[1,*]
[1]Departments of Chemistry, University of Virginia, Charlottesville, VA 22901
* Corresponding author
Email: bjv2n@virginia.edu

Keywords: Carbon-Fiber Microelectrodes, Fast-Scan Cyclic Voltammetry, Photoelectric Effect, Dopamine

View Article Online
DOI: 10.1039/D6AY00403B

Abstract

Electrochemical measurements of neurotransmitters in tissue are often made in conjunction with optogenetic and fluorescent techniques which expose the electrode to light. Recently, our lab observed that light affects the background current of electrodes, but this effect has not been systematically characterized. Here, we investigate the effects of blue and green-light exposure on carbon-fiber microelectrodes (CFMEs) using fast-scan cyclic voltammetry (FSCV). The effects of light on background charging current were observed at three potentials: near the switching potential of the dopamine waveform (1.2-1.3 V), at the dopamine oxidation potential (0.6-0.7 V), and a lower potential (0.2 V). When exposed to blue light, the largest change in background current appeared near the switching potential both during calibration and also in tissue. The background change was 50% less with green light, and the largest change was still at the switching potential. Then, we exposed CFMEs to light for 1 minute and detected dopamine. CFME currents for dopamine were enhanced after blue-light exposure during calibrations and there was a 33% increase in the current for electrically stimulated dopamine in mouse nucleus accumbens core (NAcC) brain slices. We hypothesize that this enhancement is generated by photothermal effects that shrink the width of the electric double layer and alter analyte adsorption thermodynamics. Thus, to account for the effects of light in FSCV experiments, the light should be turned on 30 s before the experiment, calibrations should be performed with light for tissue experiments, and wavelengths more red-shifted should be used when possible.

View Article Online
DOI: 10.1039/D6AY00403B

Introduction

Electrochemical and optical tools have been developed for decades to study neuroscience and neurochemistry,[1] analyzing neurotransmitter dynamics in model organisms such as rodents and *Drosophila*.[2–5] Electrochemical methods such as amperometry,[6] differential pulse voltammetry (DPV),[7] and fast-scan-cyclic voltammetry (FSCV)[5] have been used to study neurochemical signaling, directly tracking neurotransmitters. However, electrochemistry is typically limited to electroactive neurotransmitters unless they are modified with enzymes or aptamers.[8] Alternatively, optical tools such as fluorescence microscopy[9] and fiber photometry[10,11] have extended neurochemical measurements beyond electroactive molecules but are still limited as complex, specific fluorescence probes must be developed and validated for each molecule of interest.[12,13] Most novel fluorescent sensors that track neurotransmitters, such as GRAB sensors, dLight, and iGluSnFR, are based on green-fluorescent protein (GFP) which absorbs blue light.[12,14–16] Multiplexing electrochemical and optical tools extends the capabilities of each technique and allow more molecules to be measured simultaneously.[9,17–19] However, one problem with simultaneous measurements is that shining light on electrodes could lead to interferences due to photoelectric or photothermal effects.[1,4,20,21]

Recently, our lab has conducted multiplexed FSCV electrochemical measurements with several optical techniques, such as optogenetics[4,20] or fluorescence microscopy.[9,17,19] In optogenetic experiments, exogenous light-activated ion channels are expressed that stimulate the release of neurotransmitters with light.[4,20,22] First generation channelrhodopsin optogenetic channels responded to blue light, which produced an observable, measurable photocurrent upon light exposure to the surface of a carbon-fiber working electrode.[4,20] Changing to second-generation CsChrimson channels, which respond to red light, alleviated the problem, as red light does not produce a photocurrent. Most fluorescence experiments with GFP or genetically-encoded sensors also require blue-light stimulation. Unlike optogenetics experiments, during

View Article Online
DOI: 10.1039/D6AY00403B

microscopy experiments, biological samples are exposed to light for longer periods up to a few minutes. This increase in exposure time contributes to potential photochemical effects that may confound electrochemical results. For co-detection of neurotransmitters with FSCV and genetically-encoded sensors, the light for fluorescence is usually turned on 30 s before electrochemistry is acquired, to allow for the relaxation of background current changes, but that number is empirically determined at best.[4,9,17,19,20] There has not been a systematic study of photocurrents from light exposure and how wavelength and the presence of tissue affect electrochemistry.[4,20]

Photocurrents from light exposure can be produced through photoelectric or photothermal effects.[21,23–25] Both photoelectric and photothermal effects have been implicated in research areas such as optogenetics,[4,20] imaging,[9] bioelectronics,[26,27] and even catalysis.[28] The photoelectric effect occurs when light above a threshold energy called the work function hits a material, which causes electrons to be ejected from that material. However, it is unlikely that the photoelectric effect is the primary driver of photocurrents observed from CFMEs as the work function of glassy carbon ($\Phi \sim 4.6$ eV) is higher than the energy of blue light (2–3.3 eV).[29,30] Photothermal effects arise from light absorption that causes localized heating at the surface of a material.[1,21] Photothermal effects influence interfacial electrochemical processes by altering mass transport, adsorption energetics, or the properties of the electrical double layer.[24,25] As photothermal effects are work function independent, they are likely the cause of observed photocurrents at CFMEs under blue light.

The purpose of this work is to characterize how different wavelengths of light cause changes in background charging and Faradaic currents at carbon-fiber microelectrodes, especially in biological tissues. We used a broadband LED light source with two wavelength filters: blue or green. Blue light caused a larger effect than green light on CFME charging currents, especially near the switching potential. In addition, blue-light exposure for one minute increased

View Article Online
DOI: 10.1039/D6AY00403B

the current for dopamine during calibration and in brain slice tissue. Thus, this work demonstrates that light from optical experiments, especially blue light, causes changes at carbon-fiber microelectrodes but that optical and electrochemical measurements can be conducted simultaneously if one accounts for the effects of light on microelectrodes.

Methods

Chemicals and Materials

Stock solutions (10 mM) were made for dopamine (ThermoFisher Scientific, Waltham, WA) in perchloric acid (0.1 M). Dilute solutions for testing (1 μM) were made in αCSF buffer (125 mM NaCl, 2.5 mM KCl, 1.25 mM NaH_2PO_4, 25 mM $NaHCO_3$, 1 mM $MgCl_2$, 25 mM glucose, and 2 mM $CaCl_2$, pH 7.4) with individuals reagents purchased from Sigma-Aldrich (St. Louis, Missouri).

Light Source

A SOLA Light Engine (Lumencor; Beaverton, Oregon) connected to a widefield fluorescence microscope was used to produce the light used for all experiments. The SOLA works as a solid-state source of white light, which is then limited to specific wavelengths of light by inserting filters in the path of the light. The filters used in this work correspond to our attributed colors of “Blue” (MDF-GFP) and “Green” (MDF-TRITC); filters were purchased from ThorLabs (Newton, New Jersey). Power measurements were obtained using a Coherent LaserCheck Power Meter (Coherent Corp.; Saxonburg, Pennsylvania).

Acute Brain Slice Preparation

All animal experiments were performed following protocols approved by the Animal Care and Use Committee (ACUC) of the University of Virginia, which is AALAC certified. All national and institutional guidelines were followed for the animal welfare and for animal experiments. To prepare acute nucleus accumbens slices (AP +1.21; ML +1.00; DV 4.55 from the bregma), animals

View Article Online
DOI: 10.1039/D6AY00403B

were anesthetized by isoflurane and decapitated. The brain was removed and immersed in cold (0-4 °C), oxygenated (95% O_2, 5% CO_2) αCSF buffer. 400 μm-thick coronal slices were cut from the brain using a Leica VT1000 S vibratome (Teaneck, New Jersey). Slices were equilibrated in oxygenated αCSF buffer at a temperature of 37.0±0.5 °C for ~0.5 hr prior to data acquisition. During data acquisition, the brain slices were submerged in an optically-accessible chamber, continuously perfused with oxygenated αCSF buffer with a solution exchange half-time of about 6 seconds; temperature of the bath was held at 34.0±0.5 °C. Dopamine release was induced using electrical stimulation. A bipolar stimulating electrode was implanted (Biphasic Stimulus Isolator, Microprobes) in the nucleus accumbens. To evoke dopamine release, 12 biphasic stimulation pulses were applied, with currents of 300 μA and duration 4 ms, every five minutes.

Fast-scan Cyclic Voltammetry

Fast-scan cyclic voltammetry (FSCV) measurements were obtained using carbon-fiber microelectrodes (CFMEs) positioned in the Nucleus Accumbens Core (NAcc). T-650 Carbon fibers with a diameter of 7 μm (Cytec Engineering Materials Inc, Tempe, AZ), which were aspirated into a glass capillary (1.2 mm OD and 0.68 mm ID, A-M system, Sequim, WA) and pulled into electrodes with a PE-22 puller (Narishige International USA Inc, Amityville, NY). The carbon fiber was trimmed to approximately 100 μm in length from the pulled glass tip. To detect dopamine electrochemically, a triangular waveform was applied with a holding potential of -0.4 V and a switching potential of 1.3 V at 400 V/s at 10 Hz using a WaveNeuro FSCV System (Pine Research Instrumentation, Durham, NC). For data collection and analysis, HDCV software (provided by R.M. Wightman, University of North Carolina) was used. 1 M KCl was injected into glass capillaries to provide an electrical connection between the potentiostat headstage and the electrodes.

Flow Cell Calibration Experiments

View Article Online
DOI: 10.1039/D6AY00403B

Dopamine solutions were flowed through a flow cell at 2 mL/min with the use of a six-port stainless steel HPLC loop injector with an air actuator (VICI Valco Instruments, Houston, TX). For these experiments, buffer was flowed by the electrode for 5 s, buffer with dopamine was flowed by the electrode for 5 s, and then buffer again flowed by the electrode for 5s. Due to the high scan rate of the dopamine waveform (400 V/s) used in this work, background currents are large and thus a background current was taken before the exposure to dopamine and signals background subtracted.

COMSOL Simulations

A transient heat transfer model was constructed in COMSOL Multiphysics 6.4 to estimate localized photothermal heating at the carbon fiber microelectrode (CFME) surface during continuous optical illumination. The CFME was modeled as a 7 μm diameter, 100 μm long carbon cylinder embedded in a bulk aqueous domain, and experimentally measured light microscope power (~4.5mW) was converted into an estimated absorbed optical power at the CFME surface that was applied as a Gaussian-distributed boundary heat source along the illuminated electrode surface. The transient heat conduction equation was solved over 60 seconds of continuous illumination, and the maximum interfacial temperature rise ($\Delta T_{\max}$) was extracted as a function of absorbed optical power. Separate absorbed power ranges 1-5 μW and 1-3 μW were used to represent blue and green light illuminations respectively.

Statistical Analysis

Statistical analyses were reported as mean ± standard error of the mean (SEM). For dopamine experiments, each slice analyzed was a single sample within a group. For dopamine flow cell experiments, each electrode analyzed was a single sample with a group. Statistical significance was set to $p<0.05$. Data were analyzed using one-way ANOVAs as well as t-tests in

View Article Online
DOI: 10.1039/D6AY00403B

GraphPad Prism software. The data for this study are available from the corresponding authors upon request.

Results and Discussion

Effect of Blue-Light Exposure on Background Current at Carbon-Fiber Microelectrodes

To determine the effects of blue-light exposure on CFMEs, we measured the change in background charging current over time while a dopamine waveform was applied to the CFME in buffer (Fig. 1). For the first 5 seconds, CFMEs were not exposed to any light; after five seconds, blue light was turned on and remained on for a period of 60 seconds. After the light was turned off, an additional 115 seconds of data was collected for 180 seconds of data total (Fig. 1A-D). The color plot (Fig. 1A) shows the current changes over time for all voltages and highlights potentials at which there is more photocurrent than others. The current changes are not due to a Faradaic current, as there is no electroactive analyte present, but instead due to the photocurrent, which changes background charging currents. Fig. 1B shows the current versus time graph at the switching, dopamine, and lower potentials before, during, and after blue-light exposure. The charging current increases during the blue light and then gradually falls off after the light is turned off. Fig. 1C shows a background-subtracted cyclic voltammogram at 65 seconds, the peak of the change in background current at the end of the light exposure. The peak near the switching potential is located on the back scan of the voltammogram at around 1.2 V. The charging current increases the most at the switching potential, which is generally the least stable part of the background charging current. Supplemental Figure 1 shows the unsubtracted background current CVs before and after light exposure.

Next, we varied the amount of time the light was on to determine the effect on the photocurrent, from 10 to 120 s of exposure. Three potentials were examined (black lines on color plot in Fig 1A) to determine the effects of blue-light exposure near the switching potential (1.2 V), the dopamine oxidation potential (0.6-0.7 V), and a lower potential (~0.2 V) (Fig. 1D). As blue-

View Article Online
DOI: 10.1039/D6AY00403B

light exposure time increases, the change in background current also increases for the switching and dopamine oxidation potential until about 60 s. However, the lower potential is relatively constant regardless of exposure time after 15 seconds. The background current change near the switching potential is more than double the magnitude of the measurements at the other potentials.

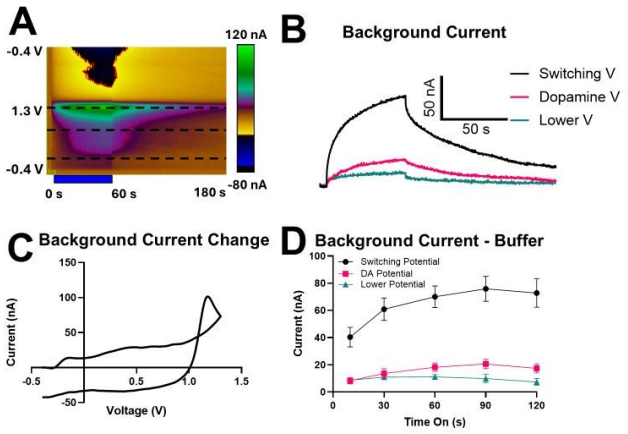

Figure 1. Blue-light exposure to carbon-fiber microelectrodes (CFMEs) produces a photocurrent which increases the background current. **(A)** Color plot of the background current change from 0 to 180 seconds. The blue bar indicates when the CFME was exposed to blue light (60 seconds). **(B)** Current vs. time graph for the background current change occurring around the switching potential (1.2), oxidation potential of dopamine (0.6 – 0.7 V), and lower potential (0.2 V). **(C)** Background (pre-light) subtracted cyclic voltammogram of the peak background current change. **(D)** Average peak current at three potentials: near the switching potential (1.2 V), dopamine oxidation potential (0.6 – 0.7 V), and a lower potential (0.2 V) at various durations of blue-light exposure (10, 30, 60, 90, and 120 seconds).

Effect of Blue-Light Exposure on Background Current at CFMEs in Tissue

Next, we characterized the effect of blue-light exposure on CFMEs that were implanted in mouse brain slices of the nucleus accumbens core. CFMEs were exposed to blue light at 5 seconds for a period of 60 seconds, and data collected for an additional 115 seconds after the light was turned off (Fig. 2A-C). The color plot shows similar changes in background charging current as in calibrations at a variety of potentials; the blue bar below the color plot shows when the CFME was exposed to blue light (Fig. 2A). The change in background current near the

View Article Online
DOI: 10.1039/D6AY00403B

switching, dopamine oxidation, and lower potentials over time in Fig. 2B shows that the background charging current increases with blue light and then decreases after the light is turned off. Fig. 2C shows the cyclic voltammogram at 65 seconds, the peak of the change in background current. The peak near the switching potential is located on the back scan of the voltammogram at around 1.2 V, with similar characteristics to blue-light exposure without tissue. Fig. 2D shows the effect of different durations of light. At the switching potential, the background charging current is maximal at 60 s, while for the dopamine potential, current continues to increase with time. At the lower potential, the background charging current change is constant while the light is on. The patterns are similar to those without tissue and the background current change at the switching potential is more than double the magnitude at the other potentials.

Fig. 2E compares the photocurrents after blue light for measurements in buffer and in tissue and there is no significant effect at either the switching potential (Paired t-test, n=6, p=0.80) or dopamine potential (Paired t-test, n=6, p=0.14) (Fig. 2E). However, there is an increase in blue light induced charging current in tissue at the lower potential (Paired t-test, n=6, p=0.035) (Fig. 2E).

There are two major potential complications when considering light effects in tissue: light penetration through tissue and possible tissue damage and oxidative stress. The first complication is the ability of the light to penetrate through tissue. Compared to other wavelengths of visible light, blue light penetrates the least through tissue due to Rayleigh scattering.[31,32] In a brain slice of only 400 μm in thickness, however, blue light is able to penetrate through the entire tissue sample, and to our CFME is implanted at the top of the tissue with a depth of about 100 μm.[33] Because similar photochemical effects are observed with tissue or without tissue, the blue light reaches the CFME in tissue, despite scattering. The second complication is the effect of blue-light exposure on biological processes in the brain. Blue-light exposure has been linked to phenomena from damaging DNA to altering neuronal firing rates.[34–36] It is unlikely, however, that these

View Article Online
DOI: 10.1039/D6AY00403B

processes would cause an immediate change in background charging current, and the signals are broad and not characteristic of sharper voltammograms that are due to neurotransmitter release. Thus, the photochemical effect is the same in tissue and is not likely due to tissue damage.

The distinct lower potential around 0.2 V does increase when CFMEs are inserted in tissue (Fig. 2E). Background shifts at this potential are often indicative of ionic changes, such as pH, changes in animals.[37] There may be more ion changes in a brain slice which would cause higher photocurrents.

Overall, these results show that the background change caused by the light stabilizes within about 30 s. Thus, in experiments where a light source is going to be used with FSCV, it is best to turn it on 30 s before the FSCV measurements, so there is a stable background to subtract with FSCV. Empirically, similar wait times had been previously used in multiplexed experiments,[9,19] but these experiments show time course of blue light effects on background.[4,9,20]

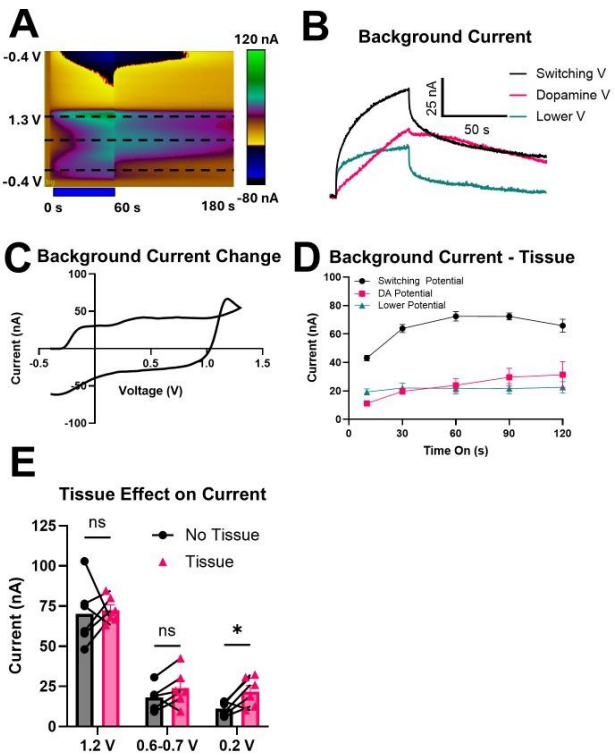

View Article Online
DOI: 10.1039/D6AY00403B

Figure 2. Blue-light exposure to carbon-fiber microelectrodes (CFMEs) implanted in mouse brain-slice tissue **(A)** Color plot of the background current change from 0 to 180 seconds. The blue bar indicates when the CFME was exposed to blue light (60 seconds). **(B)** Current vs. time graph for the background current change occurring around switching potential (1.2 V), the oxidation potential of dopamine (0.6 – 0.7 V), and the lower potential (0.2 V). **(C)** Cyclic voltammogram of the peak background current change. **(D)** Average peak current at three potentials: near the switching potential (1.2 V), dopamine oxidation potential (0.6 – 0.7 V), and the lower potential (0.2 V), at various durations of blue-light exposure (10, 30, 60, 90, and 120 seconds). **(E)** Bar graphs depicting the background current change for 60 s at the three potentials with and without tissue. (Paired t-tests, n=6, from left to right p = 0.80, p = 0.14, p = 0.035).

Color Dependence of Light on Photocurrents

After characterizing the effects of blue-light exposure on CFMEs, another wavelength of light was tested to see if the effect is dependent on wavelength (Fig. 3). Focusing on wavelengths relevant to fluorescent sensors, blue and green light were of particular interest as they excite common green and red fluorophores, respectively. For blue, a GFP filter was used with an excitation band of 469 ± 17.5 nm; for green tetramethylrhodamine Isothiocyanate (TRITC) filter was used with an excitation band of 542 ± 10 nm. Next, the power of the light was recorded to ensure the light output was the same for all colors. Supplemental Figure 2shows that each color of light output roughly 4.5 mW and were not significantly different from each other (t-Test, n = 3, p = 0.41).

Fig 3A shows the difference between blue- and green-light exposure near the switching potential in buffer (~1.2 V). Blue light caused more change in the background current when compared to green light, causing double the magnitude current compared to green light for most time points. Similar to the effects of blue light, the background current change around the dopamine oxidation potential (0.6-0.7) for green light was smaller than at the switching potential (Fig. 3B). Likewise, at the lower potential, the background current change was smaller than at the switching potential and remained fairly constant regardless of exposure time (Fig. 3C).

After observing the change in background current due to two different colors of light, the tests were repeated in tissue to observe if tissue effects would cause a difference (Fig 3D-F).

View Article Online
DOI: 10.1039/D6AY00403B

Again, blue light caused the more apparent change in background current near the switching potential (Fig. 3D). The trend is similar for the dopamine oxidation potential, where blue light is slightly more effective at changing the background current than green (Fig. 3E). Finally, the lower potential also had relatively constant changes in background current in tissue, regardless of exposure time to a light source (Fig. 3F).

Background changes near the dopamine oxidation potential were compared for 60 s of light exposure (Fig. 3G). Both colors of light change the background current and blue-light exposure increased the background current significantly more than green-light exposure (One-Way ANOVA, n=6, p = 0.0087). Figure 3H compares the background current change in tissue after 60 seconds of light exposure for the blue- and green-light exposure. Similar results were found for background current change observed in tissue, where blue-light exposure increased the background current significantly more than green-light exposure (Paired t-test, n=6, p = 0.0164).

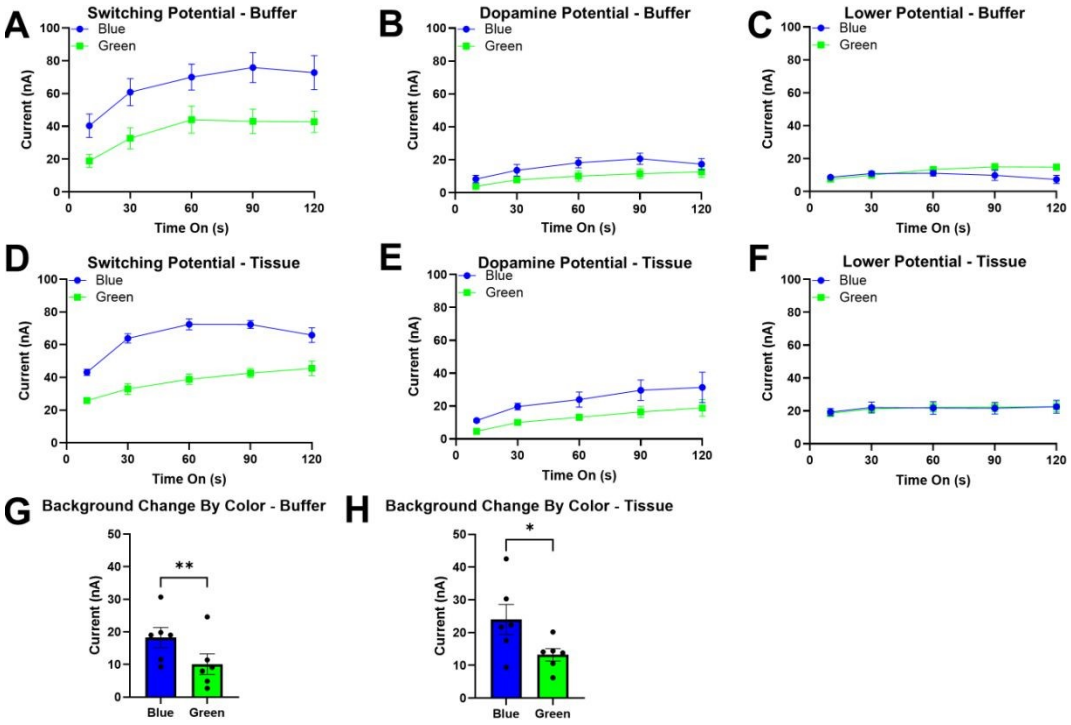

View Article Online
DOI: 10.1039/D6AY00403B

Figure 3. Color dependence on the photocurrent-induced background change. **(A-C)** Average peak current from blue and green light at three potentials: **(A)** near the switching potential (1.2 V), **(B)** dopamine oxidation potential (0.6 – 0.7 V), and **(C)** the lower potential (0.2 V) at various durations of light exposure (10, 30, 60, 90, and 120 seconds). **(D-F)** Average peak current at CFMEs implanted in tissue: **(D)** near the switching potential (1.2 V), **(E)** dopamine oxidation potential (0.6 – 0.7 V), and **(F)** the lower potential (0.2 V) at various durations of light exposure (10, 30, 60, 90, and 120 seconds). **(G)** Comparison of background current change at the oxidation potential of dopamine in buffer by color (Paired t-test, n=6, p=0.0087). **(H)** Comparison of the background current change near the oxidation potential of dopamine in tissue by color (Paired t-test, n=6, p=0.0164).

Blue-Light Exposure Enhances Dopamine Sensitivity

After observing the changes in background current under blue-light exposure, the effects of blue-light exposure on dopamine detection were determined (Fig. 4). Figure 4A shows a characteristic cyclic voltammogram of dopamine detected using flow injection analysis for calibration. After exposing the electrode to boluses of 1 μM of dopamine three times, the CFME was placed under blue light for 60 seconds, and then immediately tested with a bolus of dopamine again three times. Blue light enhances the oxidation current for dopamine without shifting the peak potentials. Figure 4B shows that dopamine signals significantly increased by 22% after 1 minute of light exposure (paired t-test, n=5, p = 0.0038). The observed enhancement of dopamine persists for about a minute after blue-light exposure as the CFMEs were not exposed to blue light during the flow injection measurements.

After observing that blue-light exposure enhanced the detection of dopamine in buffer, the same effect was tested in mouse brain slice tissue (Fig.4C-D). Dopamine was measured from the NAcC region of the mouse brain by electrically stimulating the slice once every 5 minutes. Three control stimulations of dopamine were collected without blue-light exposure and then three dopamine stimulations collected at the end of a 60 s blue-light exposure. While blue-light exposure may increase slower tonic firing rate,[38] it is not expected to alter electrically-stimulated, phasic neuronal firing.[1] Figure 4C shows stimulated dopamine release current is increased after 1 minute of light exposure without shifting the peak voltages. Figure 4D shows dopamine significantly increases by 33% after blue-light exposure in the NAcC of mouse brain slice tissue

View Article Online
DOI: 10.1039/D6AY00403B

(Paired t-test, n=8, $p < 0.0001$). To determine persistence of the blue light effect, stimulations were repeated 5 minutes apart, with one pre-light stimulated, the second stimulation at the end of 60 s of blue-light exposure, and subsequent stimulations collected for a total of 20 minutes without additional light exposure. Figure 4E shows the dopamine signal was greatest for the second stimulation right after the blue light was applied to the tissue, but there was still residual enhancement after the exposure that decreased until leveling off after 15 minutes.

The data collectively shows that dopamine detection increases in both buffer and mouse brain slice tissue after 1 minute of blue-light exposure. Consistent with our previous optogenetics data,[4,20] the increased dopaminergic current is due to the enhancement of the CFME rather than the effect of blue-light exposure on tissue itself, particularly when considering the parallel effects with and without tissue. These results show for the first time that dopamine currents are larger when exposed to light and suggest that calibrations for multiplexed experiments should account for this by calibrating the electrode in the presence of light. While 30 s will stabilize the background current changes, changes in dopamine current were persistent and small effects were seen even 5 minutes after the light was turned off, despite repeated stimulations being stable in slices with 5 minutes repetition times.[39] Most experiments either have the light present for all of the stimulations, but this data will allow a better interpretation of data collected in multiplexed optical and FSCV experiments.

View Article Online
DOI: 10.1039/D6AY00403B

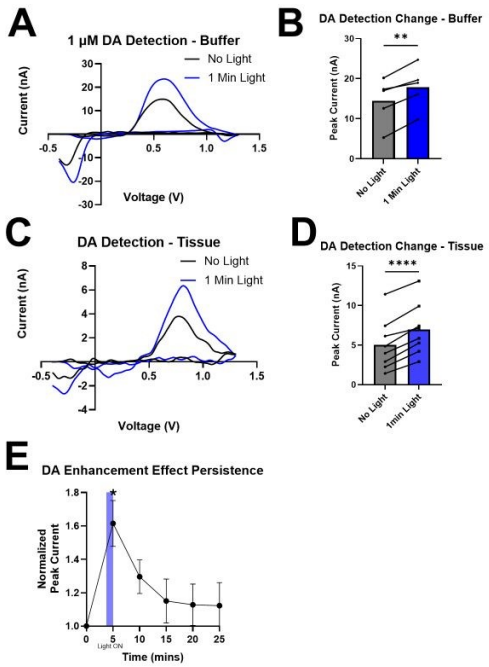

Figure 4. The effect of blue-light exposure on dopamine detection. **(A)** Cyclic voltammograms for dopamine detected in buffer without (black) and with (blue) blue-light exposure. **(B)** Bar graphs showing the change in dopamine current with (blue) and without (black) blue-light exposure during a calibration in buffer (Paired t-Test, n=5, p = 0.0038). **(C)** Cyclic voltammograms for dopamine detected in the mouse NAcC without (black) and with (blue) 1 minute of blue-light exposure. **(D)** Bar graphs show the change in dopamine current with (blue) and without (black) blue-light exposure in the mouse NAcC (Paired t-test, n=8, p < 0.0001). **(E)** Persistence of blue light effect. The blue bar indicates when light was turned on before the second stimulated dopamine release recording. Four more stimulations were collected 5 minutes apart without light. Starred point indicated statistical significance from initial stimulation (One-Way ANOVA, n=6, p = 0.0033).

Physical Interpretation of the Results

One hypothesis for the origin of the photocurrent at the microelectrode is the photoelectric effect.[4,20] Physically, however, this interpretation is not tenable as the work function for a CFME (~3.5-4 eV in solution) is considerably higher than the energy of visible blue light (2-3 eV), so electrons are likely not ejected.[40,41] Green light had less of an effect than blue, which suggests that with higher wavelengths, such as red light, effects would be even more minimal.[4,20] Thus, the observed changes in background current have two possible origins: (1) a change in the electrical double layer due to photothermal effects.[42,43] (2) a change in surface oxide functional groups on the CFME[44].

View Article Online
DOI: 10.1039/D6AY00403B

Photothermal effects on the electrical double layer are an important component of the overall mechanism, and COMSOL simulations both support and constrain this interpretation.[24,42,45] We performed COMSOL simulations of the local temperature rise around the 7 μm diameter CFME sidewall (Fig. S3) used a Gaussian-distributed boundary heat source to simulate optical absorption during illumination. Blue-light exposure produced a greater temperature rise than green-light exposure (Fig. S3A vs. S3B), but both responses were sub-Kelvin and confined to the Stern layer immediately next to the electrode surface, with the difference between wavelengths amounting to only ~20%. Simulations of optogenetics with fiber photometry show a bit larger temperature change in tissue because of the focused light, but are still on the order of a few K.[46,47] This quantitative similarity between green and blue wavelengths suggests that differential photothermal heating alone cannot account for the more-than-twofold difference in electrochemical response between blue and green illumination. Photothermal effects therefore likely serve as an amplifying rather than primary mechanism. Electron-phonon relaxation of photoexcited carbon states transfers absorbed optical energy into lattice vibrations,[48] which couple to Stern layer ion and solvent dynamics, transiently compressing the double layer and increasing capacitance and background charging current.[24,43,49] This process scales with absorbed power at any visible wavelength, consistent with green light producing a smaller but real effect, but would not by itself generate the observed wavelength selectivity.

The additional frequency dependence requires a wavelength-selective process, and a likely candidate is absorption by carbon surface oxide functional groups.[44,50,51] Enrichment of hydroxyl groups on the surface of CFMEs leads to an increase in dopamine detection,[44] and exposure to blue light leads to bond cleavage and enhanced hydroxyl groups on the surface of the CFME.[52] The mechanism of changes is carbon bond cleavage and then reactions with water, which is similar to effects seen when the electrode is scanned to voltages of 1.3 V or greater, but would be accelerated by the thermal energy of the LED light source.[21,53] Quinone and carbonyl

View Article Online
DOI: 10.1039/D6AY00403B

groups on the CFME surface have optical absorption bands peaking in the UV and blue (~350–470 nm) through n→π* and π→π* transitions, with substantially lower adsorption at green wavelengths.[54,55] Excitation of these surface groups by blue light could transiently modulate adsorption site availability and local electron density at the electrode-electrolyte interface without requiring permanent bond cleavage. The absence of sustained changes in background current at potentials characteristic of surface oxide groups (~0 V, Fig. S1) argues against irreversible oxide group accumulation,[44] but is compatible with a reversible photochemical perturbation of existing surface groups that dissipates when illumination ceases. Taken together, the COMSOL thermal modeling and the electrochemical wavelength dependence point to surface oxide photochemistry as the primary driver of the blue/green differential, with photothermal EDL compression as a secondary, wavelength-nonspecific amplifier.

The enhancement of dopamine sensitivity under blue light likely reflects the same, coupled mechanism operating on adsorption rather than capacitance. Photothermal elevation of local temperature reduces adsorption barriers and increases near-surface diffusion of dopamine,[25,53] both effects that follow the Stokes-Einstein relationship between diffusion and temperature and are present for any illumination wavelength in proportion to absorbed power. [56] The preferential sensitivity enhancement under blue light beyond what thermal modeling predicts, however, points to an additional contribution from wavelength-selective surface state excitation. Blue-light excitation of surface oxide groups may transiently increase the availability or reactivity of hydroxyl adsorption sites, consistent with prior reports that hydroxyl group enrichment specifically enhances dopamine detection, without the permanent bond cleavage associated with high-voltage electrochemical conditioning. There may also be enhanced vibrational motion within surface functional groups that transiently modulates adsorption sites.[57] While FSCV is an adsorption-controlled technique, the enhanced near-surface diffusion of dopamine would increase analyte replenishment during repeated voltametric scans.[5,58] The net result is that blue-

View Article Online
DOI: 10.1039/D6AY00403B

light exposure produces a transient but functionally significant increase in both the adsorption and the near-surface replenishment rate of dopamine at the CFME, through mechanisms that are wavelength-specific photochemical and thermodynamic mechanisms.

Conclusions

In this work, we explored the effects of blue-light exposure on CFMEs in a standard widefield fluorescence microscopy setup. We characterized the effects of light exposure on CFMEs using FSCV during calibration and in tissue. The voltages closest to the switching potential demonstrate the largest change in background current, which is likely due to phonon-mediated vibrational excitation at the CFME interface.[44,59,60] At lower potentials near 0.2 V, the effect is smaller and might result from the tightening of the width of the electric double layer.[24,42,43] Background charging currents change similarly due to blue-light exposure in brain slices, with increased changes at the lower potential. Color dependence was also studied, and the effect is larger for blue light than green light. Blue-light exposure enhances the detection of dopamine in vitro and in tissue. Thus, these results give guidelines for experiments that combine optogenetics or fluorescence with electrochemistry. The background current should be given 20-30 s to stabilize when blue light is turned on. Longer wavelengths of light such as those used for red-light optogenetics or red-shifted fluorophores should be used when possible to minimize effects. Finally, the effects of light exposure on dopamine release should be corrected with calibrations under light exposure.

Acknowledgments. This work was funded by R01NS121014 and R01NS125663.

Supplemental Information. There are 3 supporting figures. Fig. S1 Background cyclic voltammograms with and without light during calibration and in tissue. Fig. S2 Power

View Article Online
DOI: 10.1039/D6AY00403B

measurements for different light wavelengths. Fig. S3 COMSOL simulations of localized photothermal heating at the carbon-fiber microelectrode (CFME) interface during optical illumination.

References

1 T. D. Y. Kozai and A. L. Vazquez, *J. Mater. Chem. B*, 2015, **3**, 4965–4978.
2 M. Markicevic, I. Savvateev, C. Grimm and V. Zerbi, *Transl Psychiatry*, 2021, **11**, 457.
3 S. Dunst and P. Tomancak, *Genetics*, 2019, **211**, 15–34.
4 E. Privman and B. J. Venton, *Journal of Neurochemistry*, 2015, **135**, 695–704.
5 B. J. Venton and Q. Cao, *Analyst*, 2020, **145**, 1158–1168.
6 M. Benoit-Marand, M.-F. Suaud-Chagny and F. Gonon, in *Electrochemical Methods for Neuroscience*, eds. A. C. Michael and L. M. Borland, CRC Press/Taylor & Francis, Boca Raton (FL), 2007.
7 W. Li, L. Ding, Q. Wang and B. Su, *Analyst*, 2014, **139**, 3926–3931.
8 L. C. Kimble, J. S. Twiddy, J. M. Berger, A. G. Forderhase, G. S. McCarty, J. Meitzen and L. A. Sombers, *ACS Sens.*, 2023, **8**, 4091–4100.
9 K. Shrestha, Y. Chang, Y. Zhang and B. J. Venton, *Journal of Neurochemistry*, 2025, **169**, e70147.
10 M. F. Bridge, L. R. Wilson, S. Panda, K. D. Stevanovic, A. C. Letsinger, S. McBride and J. D. Cushman, *Neurophotonics*, 2024, **11**, 014305.
11 E. H. Simpson, T. Akam, T. Patriarchi, M. Blanco-Pozo, L. M. Burgeno, A. Mohebi, S. J. Cragg and M. E. Walton, *Neuron*, 2024, **112**, 718–739.
12 J. S. Marvin, B. G. Borghuis, L. Tian, J. Cichon, M. T. Harnett, J. Akerboom, A. Gordus, S. L. Renninger, T.-W. Chen, C. I. Bargmann, M. B. Orger, E. R. Schreiter, J. B. Demb, W.-B. Gan, S. A. Hires and L. L. Looger, *Nat Methods*, 2013, **10**, 162–170.
13 A. Aggarwal, R. Liu, Y. Chen, A. J. Ralowicz, S. J. Bergerson, F. Tomaska, B. Mohar, T. L. Hanson, J. P. Hasseman, D. Reep, G. Tsegaye, P. Yao, X. Ji, M. Kloos, D. Walpita, R. Patel, M. A. Mohr, P. W. Tillberg, GENIE Project Team, L. L. Looger, J. S. Marvin, M. B. Hoppa, A. Konnerth, D. Kleinfeld, E. R. Schreiter and K. Podgorski, *Nat Methods*, 2023, **20**, 925–934.
14 F. Sun, J. Zeng, M. Jing, J. Zhou, J. Feng, S. F. Owen, Y. Luo, F. Li, H. Wang, T. Yamaguchi, Z. Yong, Y. Gao, W. Peng, L. Wang, S. Zhang, J. Du, D. Lin, M. Xu, A. C. Kreitzer, G. Cui and Y. Li, *Cell*, 2018, **174**, 481–496.
15 J. Wan, W. Peng, X. Li, T. Qian, K. Song, J. Zeng, F. Deng, S. Hao, J. Feng, P. Zhang, Y. Zhang, J. Zou, S. Pan, M. Shin, B. J. Venton, J. J. Zhu, M. Jing, M. Xu and Y. Li, *Nature neuroscience*, 2021, **24**, 746–752.
16 T. Patriarchi, J. R. Cho, K. Merten, M. W. Howe, A. Marley, W.-H. Xiong, R. W. Folk, G. J. Broussard, R. Liang, M. J. Jang, H. Zhong, D. Dombeck, M. von Zastrow, A. Nimmerjahn, V. Gradinaru, J. T. Williams and L. Tian, *Science*, 2018, **360**, eaat4422.
17 Y. Zhang, P. Zhang, M. Shin, Y. Chang, S. B. G. Abbott, B. J. Venton and J. J. Zhu, *Mol Psychiatry*, 2025, **30**, 3430–3442.
18 E. D. Donarski, S. S. Connors and B. J. Venton, *Neurochem Int*, 2026, **195**, 106148.

View Article Online
DOI: 10.1039/D6AY00403B

19 L. Huang, Y. Chang, Z. Yang, W. J. Lynch and B. J. Venton, *Science Advances*, 2025, **11**, eadx6367.
20 P. Pyakurel, E. Privman Champaloux and B. J. Venton, *ACS Chem. Neurosci.*, 2016, **7**, 1112–1119.
21 X. Cui, Q. Ruan, X. Zhuo, X. Xia, J. Hu, R. Fu, Y. Li, J. Wang and H. Xu, *Chem. Rev.*, 2023, **123**, 6891–6952.
22 K. Deisseroth, *Nature Methods*, 2011, **8**, 26–29.
23 A. Einstein, *Annalen der Physik*, 1905, **322**, 132–148.
24 K. Bohinc, V. Kralj-Iglič and A. Iglič, *Electrochimica Acta*, 2001, **46**, 3033–3040.
25 X. Zhao and D. Vanderbilt, *Phys. Rev. B*, 2002, **65**, 075105.
26 E. Joseph, M. Ciocca, H. Wu, S. Marcozzi, M. A. Ucci, K. Keremane, L. Zheng, B. Poudel, C. Wu, A. Camaioni, K. Wang, S. Priya and T. M. Brown, *npj Biosensing*, 2024, **1**, 15.
27 K. Chen, B. Wu, D. Krahe, A. Vazquez, J. R. Siegenthaler, R. Rechenberg, W. Li, X. T. Cui and T. D. Y. Kozai, *Advanced Functional Materials*, 2024, **34**, 2403164.
28 H. Huang, K. A. Steiniger and T. H. Lambert, *J. Am. Chem. Soc.*, 2022, **144**, 12567–12583.
29 R. Schletti, P. Wurz and T. Fröhlich, *Rev. Sci. Instrum.*, 2000, **71**, 499–503.
30 O. E. Glukhova and M. M. Slepchenkov, *J. Phys. Chem. C*, 2016, **120**, 17753–17758.
31 S. Senova, I. Scisniak, C.-C. Chiang, I. Doignon, S. Palfi, A. Chaillet, C. Martin and F. Pain, *Sci Rep*, 2017, **7**, 43997.
32 S. R. V. Leeuwen and G. V. G. Baranoski, *JBO*, 2018, **23**, 025001.
33 C. T. Inglut, B. Gaitan, D. Najafali, I. A. Lopez, N. P. Connolly, S. Orsila, R. Perttilä, G. F. Woodworth, Y. Chen and H.-C. Huang, *Photochem Photobiol*, 2020, **96**, 301–309.
34 Z. Lin, G. Hou, Y. Yao, Z. Zhou, F. Zhu, L. Liu, L. Zeng, Y. Yang and J. Ma, *Front. Hum. Neurosci.*, DOI:10.3389/fnhum.2021.739333.
35 T. R. Nash, E. S. Chow, A. D. Law, S. D. Fu, E. Fuszara, A. Bilska, P. Bebas, D. Kretzschmar and J. M. Giebultowicz, *npj Aging Mech Dis*, 2019, **5**, 8.
36 K. M. Tyssowski and J. M. Gray, *eNeuro*, DOI:10.1523/ENEURO.0085-19.2019.
37 P. Takmakov, M. K. Zachek, R. B. Keithley, E. S. Bucher, G. S. McCarty and R. M. Wightman, *Anal. Chem.*, 2010, **82**, 9892–9900.
38 K. J. Fogle, K. G. Parson, N. A. Dahm and T. C. Holmes, *Science*, 2011, **331**, 1409–1413.
39 C. E. John and S. R. Jones, in *Electrochemical Methods for Neuroscience*, eds. A. C. Michael and L. M. Borland, CRC Press/Taylor & Francis, Boca Raton (FL), 2007.
40 H. Ago, T. Kugler, F. Cacialli, W. R. Salaneck, M. S. P. Shaffer, A. H. Windle and R. H. Friend, *J. Phys. Chem. B*, 1999, **103**, 8116–8121.
41 S. Barazzouk, S. Hotchandani, K. Vinodgopal and P. V. Kamat, *J. Phys. Chem. B*, 2004, **108**, 17015–17018.
42 Y. S. Park and I. S. Kang, *Journal of Electroanalytical Chemistry*, 2021, **880**, 114923.
43 C. M. Schott, P. M. Schneider, K.-T. Song, H. Yu, R. Götz, F. Haimerl, E. Gubanova, J. Zhou, T. O. Schmidt, Q. Zhang, V. Alexandrov and A. S. Bandarenka, *Chem. Rev.*, 2024, **124**, 12391–12462.
44 J. G. Roberts, B. P. Moody, G. S. McCarty and L. A. Sombers, *Langmuir*, 2010, **26**, 9116–9122.
45 J. J. López-García, J. Horno and C. Grosse, *Current Opinion in Colloid & Interface Science*, 2016, **24**, 23–31.

View Article Online
DOI: 10.1039/D6AY00403B

46 A. Picot, S. Dominguez, C. Liu, I.-W. Chen, D. Tanese, E. Ronzitti, P. Berto, E. Papagiakoumou, D. Oron, G. Tessier, B. C. Forget and V. Emiliani, *Cell Reports*, 2018, **24**, 1243-1253.e5.
47 G. Arias-Gil, F. W. Ohl, K. Takagaki and M. T. Lippert, *Neurophotonics*, 2016, **3**, 045007.
48 A. C. Ferrari and J. Robertson, *Phys. Rev. B*, 2000, **61**, 14095–14107.
49 A. J. Bard and L. R. Faulkner, *Electrochemical methods: fundamentals and applications*, John Wiley and Sons, New York, 2001.
50 B. D. Bath, H. B. Martin, R. M. Wightman and M. R. Anderson, *Langmuir*, 2001, **17**, 7032–7039.
51 K. T. Kawagoe, J. B. Zimmerman and R. M. Wightman, *Journal of Neuroscience Methods*, 1993, **48**, 225–240.
52 S. Siahrostami, G.-L. Li, V. Viswanathan and J. K. Nørskov, *J. Phys. Chem. Lett.*, 2017, **8**, 1157–1160.
53 Z. Ge, D. G. Cahill and P. V. Braun, *Phys. Rev. Lett.*, 2006, **96**, 186101.
54 E. H. Anouar, C. P. Osman, J.-F. F. Weber and N. H. Ismail, *Springerplus*, 2014, **3**, 233.
55 A. D. Modestov, J. Gun and O. Lev, *Surface Science*, 1998, **417**, 311–322.
56 Q. Jia, C. Yang, B. J. Venton and K. H. DuBay, *Chemphyschem*, 2022, **23**, e202100783.
57 C. Yang, E. Trikantzopoulos, C. B. Jacobs and B. J. Venton, *Anal Chim Acta*, 2017, **965**, 1–8.
58 B. D. Bath, H. B. Martin, R. M. Wightman and M. R. Anderson, *Langmuir*, 2001, **17**, 7032–7039.
59 Y. Chang and B. J. Venton, *Anal Methods*, 2020, **12**, 2893–2902.
60 F. Herold, S. L. Guldahl-Ibouder, T. Hein, P. Schühle and M. Rønning, *Applied Catalysis A: General*, 2025, **694**, 120165.

View Article Online
DOI: 10.1039/D6AY00403B

Data Availability Statement for:

Blue Light Enhances Background Current and Dopamine Sensitivity of Carbon-Fiber Microelectrodes During Fast-Scan Cyclic Voltammetry

Eric D. Donarski[1], David R. Luedeka[1], and B. Jill Venton[1,*]
[1]Departments of Chemistry, University of Virginia, Charlottesville, VA 22901
* Corresponding author
Email: bjv2n@virginia.edu

Data for this article, including raw .hdcv files of FSCV experiments and processed data in Microsoft Excel and/or Graphpad Prism are available at University of Virginia – Dataverse Libra at https://doi.org/10.18130/V3/CSSH1Y .